tend to increase the binding strength.

## Conclusions

Electrostatics and ion binding cause strong interactions between diffusional flows of charged proteins and supporting electrolytes. Owing to the large difference in the mobilities of protein ions and typical counterions, a gradient in the concentration of a charged protein generates a relatively strong electric field to prevent charge separation. The diffusion-induced electric field along the protein gradient produces a coupled flow of the ions of the supporting electrolyte. Neglect of the simultaneous flow of the supporting electrolyte can lead to a systematic error in the measured diffusivity of the protein. Multicomponent diffusion coefficients for the mixtures can be estimated as functions of the pH, ionic strength, and protein concentration provided the diffusivities of the species and the number of bound ions are known.

*Acknowledgment.* The author thanks G. Samardzic for technical assistance. Acknowledgment is made to the Natural Sciences and Engineering Research Council for financial support of this research.

**Registry No.** NaCl, 7647-14-5.

# Salt-Induced Conformational Changes in DNA: Analysis Using the Polymer RISM Theory

**Fumio Hirata and Ronald M. Levy***

*Department of Chemistry, Rutgers University, New Brunswick, New Jersey 08903* *(Received: May 9, 1988)*



A RISM theory developed for solvated polymers is applied to polyelectrolyte solutions modeled as an infinite helical array of charged spheres immersed in a primitive-type electrolyte solution. The relation to earlier theories by Manning and Iwasa based on the same model is studied. As an application of the theory, salt effects on conformations of DNA in solution are examined over a wide range of added salt concentrations. It is found that the counterion distribution around the phosphates is not solely determined by the axial charge density of the polyion but depends on a more detailed characterization of the polyion charge distribution. A calculation is performed for the free energy dependence of B- and Z-DNA helical forms on salt concentration over a wide range of added salt concentration. A transition in the stable DNA form from B- to Z-DNA is predicted at ~3.6 M added salt in qualitative accord with experiment.

## Introduction

The sustained intense interest in the physical chemistry of polyelectrolyte solutions is motivated in part by its importance in biological systems.[1] A major conceptual breakthrough in our understanding of polyelectrolytes was made by Manning with his development of an ionic strength limiting law; the associated "counterion condensation" theory is based on a simple two-state thermodynamic model.[2-4] While the theory has enjoyed a status similar to the Debye-Hückel theory for simple electrolyte solutions, it has left many questions unanswered, such as the detailed structure of counter- and co-ion atmospheres around polyions. Attempts to answer these questions and to place the theory upon a more solid statistical mechanics foundation have been made during the past decade. These include studies using the mean spherical model (MSM),[5] hypernetted chain (HNC),[6] Poisson-Boltzmann (PB),[7] and Monte Carlo (MC)[8-10] methods. With few exceptions, most theoretical studies have been carried out for a simplified model of a polyion for which charges are distributed uniformly along the cylindrical axis.[2,5,6,8,11,12] While the cylindrical rod description with a continuous charge distribution has been successfully used to describe many polyion properties,[13] models that can incorporate more realistic features of the polyion structure are of great interest. One such model, which may be described as "beads on a string", was first investigated by Rice using a Poisson-Boltzmann equation,[14] later by Manning and Zimm[15] based on the Mayer cluster expansion,[16] and by Iwasa[17] by a mode expansion.[18] The latter two methods lead to the same result for the excess chemical potential of a polyion due to interaction with small ions as a leading term of the expansions. It is of interest to develop an integral equation method for this model, because the evaluation of higher order terms after the first few terms in the expansions is generally very difficult.

A primary goal of a statistical mechanics polyelectrolyte theory is to establish the dependence of interionic distribution functions on the polyion structure. This can be achieved within the framework of the so-called RISM or site-site Ornstein-Zernike (SSOZ) equation,[19,20] which is one of the most successful statistical mechanics approaches for the study of molecular liquids in which molecules are modeled as collections of several interaction sites.[21-23]

(1) Anderson, C. F.; Record, M. T., Jr., *Annu. Rev. Phys. Chem.* **1982**, *33*, 191.
(2) Manning, G. S. *J. Chem. Phys.* **1969**, *51*, 924. *Ibid.* **1969**, *51*, 3249.
(3) Manning, G. S. *Biophys. Chem.* **1977**, *7*, 95.
(4) Manning, G. S. *Q. Rev. Biophys.* **1978**, *II*, 179.
(5) Fixman, M. *J. Chem. Phys.* **1979**, *70*, 4995.
(6) Bacquet, R.; Rossky, P. J. *J. Phys. Chem.* **1984**, *88*, 2660.
(7) Le Bret, M.; Zimm, B. H. *Biopolymers* **1984**, *23*, 287.
(8) Le Bret, M.; Zimm, B. H. *Biopolymers* **1984**, *23*, 271.
(9) Murthy, C. S.; Bacquet, R.; Rossky, P. J. *J. Phys. Chem.* **1985**, *89*, 701.
(10) Vlachy, V.; Haymet, D. J. *J. Chem. Phys.* **1986**, *84*, 5874.
(11) Fuoss, R. M.; Katchalsky, A.; Lifson, S. *Proc. Natl. Acad. Sci. U.S.A.* **1951**, *37*, 579.
(12) Kotin, L.; Nagasawa, M. *J. Chem. Phys.* **1962**, *36*, 873.
(13) Manning, G. S. *Annu. Rev. Phys. Chem.* **1972**, *23*, 117.
(14) Lapanje, S.; Haebig, J.; Davis, T.; Rice, S. A. *J. Am. Chem. Soc.* **1961**, *83*, 1590.
(15) Manning, G. S.; Zimm, B. H. *J. Chem. Phys.* **1965**, *43*, 4250.
(16) Mayer, J. *J. Chem. Phys.* **1950**, *18*, 1426.
(17) Iwasa, K. *J. Chem. Phys.* **1975**, *62*, 2967.
(18) Andersen, H. C.; Chandler, D. *J. Chem. Phys.* **1970**, *53*, 547. Chandler, D.; Andersen, H. C. *Ibid.* **1970**, *54*, 26. Andersen, H. C.; Chandler, D. *Ibid.* **1971**, *55*, 1497.
(19) Chandler, D.; Andersen, H. C. *J. Chem. Phys.* **1972**, *57*, 1930. Chandler, D. *Mol. Phys.* **1976**, *31*, 1213; *J. Chem. Phys.* **1977**, *67*, 1113.
(20) Cummings, P. T.; Stell, G. *Mol. Phys.* **1982**, *46*, 383.
(21) Lowden, L. J.; Chandler, D. *J. Chem. Phys.* **1973**, *59*, 6587; **1974**, *61*, 5228.
(22) Hirata, F.; Rossky, P. J. *Chem. Phys. Lett.* **1981**, *84*, 329. Hirata, F.; Pettitt, B. M.; Rossky, P. J. *J. Chem. Phys.* **1982**, *77*, 509. Hirata, F.; Rossky, P. J.; Pettitt, B. M. *J. Chem. Phys.* **1983**, *78*, 4133.
(23) Pettitt, B. M.; Rossky, P. J. *J. Chem. Phys.* **1982**, *77*, 1451; *J. Chem. Phys.* **1983**, *78*, 7296.

0022-3654/89/2093-0479$01.50/0 

However, the extension of the theory to polymeric systems is in general a formidable task due to the size and complication of the intramolecular correlation matrix that appears in the equation. An approximation commonly employed in this situation is the superposition approximation, which essentially decomposes multiple correlations into pair correlations, ignoring higher order correlations.[24,25] We have shown in a previous paper that for cases in which one can take advantage of molecular periodicity, the RISM equation for polyelectrolytes can be reduced to a tractable size without sacrificing the higher order correlations.[26] A similar use of periodicity to reduce the complexity of the RISM equations has also been used in other contexts.[27-29] Preliminary application to a variety of polymer–solvent systems including a linear polyion in water, for which comparison has been made with molecular dynamics simulations, has demonstrated the usefulness of this approach.[26]

One of the objectives of this article is to clarify the relation between the polymeric RISM and earlier theories based on the same model. As an application of the theory we present the results of calculations of the effect of added salt on the conformations of DNA in solution.

## Theory

We consider a simplified model of polyelectrolyte solutions in which a polyion and small mobile ions are immersed in a continuum dielectric solvent. The polyion is represented by an infinite array of charged spheres (ions) equally spaced along a linear or helical chain. Hereafter we use subscript $p$ for the polyion and $i$ and $j$ for the small ions. The interaction between a pair of ions is represented by

$$u_{Mi} = u^*_{Mi}(r) + Z_M Z_i / Dr \tag{1}$$

where $u^*_{Mi}(r)$ is a short-range interaction, $Z_M$ and $Z_i$ are the charges, $D$ is the dielectric constant of the medium, and the subscript $M$ stands for either $p$ or $j$.

For the simplified model described above, all the correlation functions between all sites on the polyion and the $i$-type small ion are identical and the RISM equation for the polyion-small ion correlation function is written as:[26]

$$h_{pi}(r) = \sum_j \{W_p * c_{pj} \delta_{ji} + W_p * c_{pj} * \rho_j h_{ji}^0(r)\} \tag{2}$$

where $h_{pi}(r)$ and $c_{pi}(r)$ are the total and the direct correlation functions for a polyion–small ion pair, respectively. $h_{ij}^0(r)$ is the total correlation function for an $i$–$j$ pair of small ions in the electrolyte solution without the polyion and $\rho_j$ is the number density of the $j$th species. The asterisks stand for convolution integrals. $W_p(r)$ is defined by

$$W_p(r) = \sum_n w_{pn}(r) \tag{3}$$

where $w_{pn}(r)$ is an intramolecular correlation function for the site pair $p$ and $n$ in the polyion and is defined by

$$w_{pn}(r) = \delta_{pn}\delta(r) + (1 - \delta_{pn})(1/4\pi L_{pn}^2)\delta(r - L_{pn}) \tag{4}$$

where $\delta_{pn}$ and $\delta(r)$ are Kronecker delta and Dirac delta functions; $L_{pn}$ is a distance between sites $p$ and $n$.

When the interaction includes the long range part as in eq 1, a common strategy involves renormalization of the long-range part to ensure convergence. The general scheme for renormalization of the RISM equations is given in ref 20. Defining the short- and long-range parts of the direct correlation function by

$$\phi_{pi} = \frac{-Z_p Z_i}{DkT}\frac{1}{r} \tag{5}$$

$$c^*_{pi} = c_{pi} - \phi_{pi} \tag{6}$$

eq 2 is rewritten as

$$h_{pi} = c^*_{pi} + \theta_{pi} + Q_{pi} \tag{7}$$

where $\theta_{pi}$ and $Q_{pi}$ are defined by

$$\theta_{pi} = \sum_j W_p * c^*_{pj} * (\delta_{ij} + \rho_j h_{ji}^0) - c^*_{pi} \tag{8}$$

$$Q_{pi} = \sum_j W_p * \phi_{pj} * (\delta_{ij} + \rho_j h_{ji}^0) \tag{9}$$

The equations must be supplemented by approximate relations for $c^*$ to be solved. The most commonly used closures are Percus–Yevick (PY) and HNC type closures:

$$c^*_{pi} = \exp[-u^*_{pi}/kT + Q_{pi}]F_{pi} - 1 - \theta_{pi} - Q_{pi} \tag{10}$$

$$F_{pi} = \exp[\theta_{pi}], \quad \text{(HNC)}$$

$$F_{pi} = 1 + \theta_{pi}, \quad \text{(PY)}$$

The set of equations (8)–(10) is solved iteratively with a given $h_{ij}^0$, the total correlation functions for the electrolyte solution without a polyion, to obtain the pair correlation function $h_{pi}$. Accuracy of the numerical procedure is conveniently checked by examining the charge neutrality condition:

$$\sum_i \rho_i Z_i \int_0^\infty h_{pi}(r) 4\pi r^2 \, \mathrm{d}r = -N_p Z_p \tag{11}$$

or a defect function for $h_{pi} - Q_{pi}$ defined by

$$\Delta_{h-Q} = \sum_i \rho_i Z_i \int_0^\infty [h_{pi}(r) - Q_{pi}(r)] 4\pi r^2 \, \mathrm{d}r \tag{12}$$

where $N_p$ is a number of ions in a polyelectrolyte chain. Following the procedure given by Bacquet and Rossky,[6] it is shown in the Appendix that $\Delta_{h-Q}$ is zero for exact $h_{pi}$ and $Q_{pi}$. The defect function provides a more useful numerical check of the solutions to the RISM equations, because numerical error associated with the integration is canceled out.

The excess chemical potential of the polyion due to the interaction with small ions can be calculated with a standard coupling parameter expression:[30,31]

$$\Delta\mu_p/kT = \sum_j \int_0^1 \mathrm{d}\zeta \int_0^\infty 4\pi r^2 u_{pj}(r)\{h_{pj}(r,\zeta) + 1\} \, \mathrm{d}r \tag{13}$$

or a more convenient expression developed by Singer and Chandler:[32,33]

$$\Delta\mu_p/kT = \sum_j \int_0^\infty 4\pi r^2 \left\{\frac{1}{2}h_{pj}^2(r) - c_{pj}(r) - \frac{1}{2}h_{pj}(r)c_{pj}(r)\right\} \mathrm{d}r \tag{14}$$

As is clear from eq 13, $\Delta\mu_p$ is the free energy change per charge group associated with the creation of a polyion in a system of small ions. It is, therefore, a measure of salt effects upon the conformations of the polyion.

It is instructive to see how the theory is related to earlier theories based on a similar model, especially, the Manning–Zimm and Iwasa theories. For this purpose, we first neglect $\theta_{pi}$, the *indirect* part of the short-range polyion–small ion correlation, in eq 7 and 10. We also approximate $h_{ij}^0$, the correlation function between small ion pairs, by the Debye–Hückel correlation function:

$$q_{ij}(r) = (-Z_i Z_j / DkT) \exp(-\kappa r)/r \tag{15}$$

where the Debye shielding parameter $\kappa$ is defined by

$$\kappa = \left\{\frac{4\pi}{DkT}\sum_i Z_i^2 \rho_i\right\}^{1/2} \tag{16}$$

(24) Pettitt, B. M.; Karplus, M. *J. Chem. Phys.* **1985**, *83*, 781; *Chem. Phys. Lett.* **1985**, *121*, 194.
(25) Soumpasis, D.-M. *Proc. Natl. Acad. Sci. U.S.A.* **1984**, *81*, 5116.
(26) Hirata, F.; Levy, R. M. *Chem. Phys. Lett.* **1987**, *136*, 267.
(27) Chandler, D.; Singh, Y.; Richardson, D. M. *J. Chem. Phys.* **1984**, *81*, 1975.
(28) Chandler, D. *Chem. Phys. Lett.* **1987**, *139*, 108.
(29) Schweizer, K. S.; Curro, J. G. *Phys. Rev. Lett.* **1987**, *58*, 246.
(30) McQuarrie, D. A. *Statistical Mechanics*; Harper and Row: New York, 1976.
(31) Chiles, R. A.; Rossky, P. J. *J. Am. Chem. Soc.* **1984**, *106*, 6867.
(32) Singer, S. J.; Chandler, D. *Mol. Phys.* **1985**, *55*, 621.
(33) Zichi, D. A.; Rossky, P. J. *J. Chem. Phys.* **1986**, *84*, 1712.

Then, eq 7 and 9 become

$$h_{pi}(r) = \exp[-u^*_{pi}(r)/kT + Q_{pi}(r)] - 1 \quad (17)$$

$$Q_{pi}(r) = \sum_j \{W_p * \delta_{ji}\phi_{pj}(r) + W_p * \phi_{pj} * \rho_j q_{ji}(r)\} \quad (18)$$

Equation 17 corresponds to Meeron's correlation function for a simple ionic solution.[34] Defining the Fourier transform of a function $f(r)$ by

$$f(\mathbf{k}) = \int_{-\infty}^{\infty} f(r) \exp(-i\mathbf{kr})\, d\mathbf{r}$$

the Fourier transform of eq 18 is given by

$$Q_{pi}(k) = W_p(k)[\phi_{pi}(k) + \sum_j \phi_{pj}(k)\rho_j q_{ji}(k)] \quad (19)$$

where $W_p(k)$, $\phi_{pi}(k)$, and $q_{ij}(k)$ are

$$W_p(k) = \sum_n \frac{\sin(kL_n)}{kL_n} \quad (20)$$

$$\phi_{pi}(k) = -\frac{4\pi}{DkT}\frac{Z_p Z_i}{k^2} \quad (21)$$

$$q_{ij}(k) = -\frac{Z_i Z_j}{DkT}\frac{4\pi}{k^2 + \kappa^2} \quad (22)$$

The inverse Fourier transform of eq 19 can be performed analytically to give

$$Q_{pi}(r) = -\frac{Z_p Z_i}{rDkT}\left\{\exp(-\kappa r) + \sum_n \left[\frac{\exp(-\kappa(r + L_n))}{L_n\kappa} + H(r - L_n)\frac{\exp(-\kappa(r - L_n))}{L_n\kappa} - H(L_n - r)\frac{\exp(\kappa(r - L_n))}{L_n\kappa}\right]\right\} \quad (23)$$

where $H(x)$ is the Heaviside function, namely

$$H(x) = 0, \quad x < 0$$

$$H(x) = 1, \quad x \geq 0 \quad (24)$$

and $L_n$ is the distance to the $n$th ion in the polyelectrolyte from the central ion. Here we make the further approximation for the correlation function, eq 17, that is

$$h_{pi} = Q_{pi}(r) \quad (25)$$

Note that a similar approximation for simple electrolyte solutions leads to the Debye–Hückel limiting law for thermodynamic properties. From eq 13, 23, and 25, taking into account the charge neutrality condition, we have

$$\Delta\mu_p = -\frac{Z_p^2}{2D}\kappa + \frac{Z_p^2}{2D}\sum_n \left\{\frac{e^{-\kappa L_n}}{L_n} - \frac{1}{L_n}\right\} \quad (26)$$

For a model in which the ions are equally spaced on a linear array, $L_n = nb$ ($b$: spacing of adjacent ions), and $\sum_n$ is replaced by $2\sum_{n=1}^{\infty}$ because there are two ions symmetrically placed around the central ion. Thus, eq 26 becomes

$$\Delta\mu = -\frac{Z_p^2}{2D}\kappa + \frac{Z_p^2}{Db}\sum_n \left\{\frac{e^{-n\kappa b}}{n} - \frac{1}{n}\right\} = -\frac{Z_p^2}{2D}\kappa + \frac{Z_p^2}{Db}\{-\ln(1 - e^{-\kappa b}) + \ln(0)\} \quad (27)$$

In the second equation we have employed the relation, $\sum_{n=1}^{\infty} x^n/n = \ln(1 - x)$. In eq 27, the first term is the charging free energy of an ion in the field produced by the small ions, while the second term arises from the existence of other ions on the polyelectrolyte. The term $(Z_p^2/2D)\ln(0)$ is a sum over all *direct* phosphate–phosphate interactions when the small ions are absent, and inclusion of the term in eq 27 is a consequence of the fact that the direct interaction is not included in eq 13. Equation 27 was originally derived by Manning and Zimm[15] as the leading term in the cluster expansion of the free energy for the "beads on a string" model of a polyelectrolyte solution; this is analogous to the "ring" approximation in the Mayer theory for simple ionic solutions.[16] The same approximation is called the "random-phase approximation"[18] in terms of the mode expansion method in Iwasa's article.[17] The equation can be derived more intuitively by summing up screened Coulombic potentials between two charges in the polyion over all possible pairs.[15] The expression is used as a key equation in Manning's condensation theory.

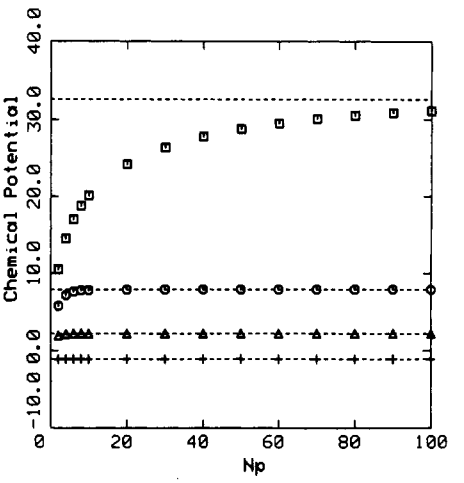


**Figure 1.** Effect of truncation of the infinite sum in eq 27: squares, $b$ = 1.0 Å and $\kappa$ = 0.0104 Å$^{-1}$ (0.001 M); circles, $b$ = 1.0 Å and $\kappa$ = 0.3287 Å$^{-1}$ (1.0 M); triangles, $b$ = 8.0 Å and $\kappa$ = 0.0104 Å$^{-1}$; crosses, $b$ = 8.0 Å and $\kappa$ = 0.3287 Å$^{-1}$. The exact values calculated from the second equation of (27) are shown by dashed lines.

It is interesting from the point of view of numerical calculations to examine the effect of finite summation in eq 23 and 26, since eq 2 is only exact within the RISM approximation when the polyion chain extends infinitely. A cutoff of the chain at finite length introduces an "end effect". This problem has been considered by us in a previous paper[26] by comparing the correlation function at certain separations for different truncation of the chains. The result exhibited rather rapid convergence to the infinite chain limit for the system considered, which has a high concentration (5 mol/L) of small ions. It is easy to see $Q_{pi}(r)$ does not diverge at any separation $r$ when $N_p$ goes to infinity unless $\kappa$ or $b$ is zero, a case we are not concerned with. It is also obvious that the rate of convergence of the function with finite $N_p$ to the infinite $N_p$ limit depends very much upon $b$ and $\kappa$. In Figure 1, $\{\Delta\mu + (Z_p^2/Db)\sum_n(1/n)\}$ with various $b$ and $\kappa$ is plotted as a function of $N_p$. As is seen, the convergence becomes slower as $b$, which is inversely proportional to the charge density of the polyion, increases and $\kappa$, which is the inverse of the Debye length (thickness of the ionic atmosphere for the small ions), becomes smaller.

While the "end effect" *mathematically* represents the approximation of an infinite system by a finite system, a *physical* macromolecule is a finite system, and a study of the dependence of the free energy on polyion length is of physical interest.[29] The approach proposed above may be employed for investigating such "polymer size" effects.

## Salt Effects on DNA Conformations

It is well established that a DNA double helix changes its conformation from B to Z forms when the ionic strength of the solution increases.[35,36] For monovalent electrolytes such as sodium chloride, the transition occurs around 2.3 mol/L.[36] As has been pointed out by other authors, the transition is not explained by the Manning condensation theory.[25,37] In the first place, it is not

(34) Meeron, E. *J. Chem. Phys.* **1958**, *28*, 630.

(35) Wang, A. H. J.; Quigley, G. J.; Kolpak, F. J.; van der Marel, G.; van Boom, J. H.; Rich, A. *Science (Washington, D.C.)* **1981**, *211*, 171.
(36) Pohl, F. M. *Cold Spring Harbor Symp. Quant. Biol.* **1983**, *47*, 113.
(37) Behe, M.; Felsenfeld, G. *Proc. Natl. Acad. Sci. U.S.A.* **1981**, *78*, 1619.

**TABLE I: Helical Parameters**

| | $R_H$, Å | $\Delta\phi_H$, deg | $\Delta Z_H$, Å | $\phi_H^0$, deg | $Z_H^0$, Å |
|---|---|---|---|---|---|
| B-DNA0 | 8.91 | 36 | 3.38 | 95.2 | 2.08 |
| B-DNA1 | 7.00 | 36 | 3.38 | 95.2 | 2.08 |
| B-DNA2 | 8.91 | 36 | 3.00 | 95.2 | 2.08 |
| B-DNA3 | 8.91 | 20 | 3.38 | 95.2 | 2.08 |

entirely clear if the theory can be applied at such high concentrations where the transition occurs. Among the difficulties in applying the Manning theory at high concentration are the neglect of small ion–small ion correlations and the neglect of the short-range interactions of the polyion with the small ions. Second, predictions based solely on the DNA axial charge density should lead to the opposite result, since the axial charge density of the Z form is lower than that of the B form. This suggests the necessity of alternative approaches that take into account a more detailed characterization of the charge distribution on the DNA helices. One such attempt has been made by Soumpasis,[25] which includes a more realistic charge distribution for B- and Z-DNA as well as elaborate correlations for small ion pairs generated by a semianalytic equation.[38] While the calculations are in good agreement with the trend experimentally observed, the theory relies on the superposition approximation, which neglects the effect of higher order intramolecular correlations on the polyion–small ion distribution functions. These correlations are expected to play a significant role in the structure of the ionic atmosphere around the polyion. Another interesting calculation has been carried out by Pack and co-workers based on the generalized three-dimensional Poisson–Boltzmann equation, in which repulsive interactions between small ions are taken into account. The result for 0.01 M salt solution indicates that the concentration of counterions at the immediate surface of the Z form is higher than for the B form despite the lower axial charge density. In the Pack calculation, the excess electrostatic interaction between phosphates and counterions in the Z form partly compensates the relative instability of the conformation in vacuo compared to the B form, although the actual transition is not observed at this concentration.

In the present study we propose an alternative approach to the problem based on the theory described in the previous section. The model employed is similar to that of Soumpasis, that is, double-stranded helices of phosphates immersed in a primitive type electrolyte solution, except for the number of phosphates. We include much larger numbers of phosphates, 480, compared to 24 in Soumpasis's work to minimize the end effects described in the previous section. The calculations are performed for five models of DNA over a wide range of salt concentrations (2–6 mol/L) at temperature 298 K. The concentration range has been chosen because the actual B-to-Z transition occurs in this region. Fortunately, it is easier to solve numerically the polymer RISM equations in this concentration range because the larger value of $\kappa$ increases the rate of convergence. To study the effect of the charge distribution around DNA upon conformation, we considered four different models for B-DNAs, which have different helical parameters and are referred to as B-DNA$i$ ($i$ = 0, 1, 2, 3). The coordinates of the phosphates in the strand are generated by using the cylindrical coordinate system:

$$x_H = R_H \cos(\phi_H + \Delta\phi_H),$$
$$y_H = R_H \sin(\phi_H + \Delta\phi_H),$$
$$z_H = z_H^0 + \Delta z_H \qquad (28)$$

where the subscript H stands for either of the two strands in the double helices. The charges are placed at the phosphates. The helical parameters $R_H$, $\phi_H$, $\Delta\phi_H$, $z_H^0$, and $\Delta z_H$ for B-DNA$i$ are listed in Table I. Those for the standard B-DNA (B-DNA0) have been taken from Arnott.[40] B-DNA1 has a smaller helix radius $R_H$ than B-DNA0, while B-DNA3 has a smaller $\Delta\phi_H$ compared to B-DNA0. Both models have a higher *volume* charge density than the standard B-DNA, although the axial charge density is the same. B-DNA2 has a shorter pitch ($\Delta Z_H$) compared to the standard B-DNA, which gives rise to the higher axial charge density. The last DNA model considered is Z-DNA, and the phosphate coordinates are obtained from the crystal structure of Wang et al.[35] A 12-6-1 type potential[26] is employed for small ion–small ion and small ion–phosphate interactions. The energy parameters are listed in Table II. Since we are interested only in the qualitative nature of salt effects on DNA conformation, no attempt has been made to optimize the parameters. The HNC-like closure is used in the calculations for correlations between small ions, while the PY-like closure is employed for the phosphate–small ion correlations because we could not achieve the convergence with the HNC closure. Numerical accuracy has been checked based on eq 11 and 12. The defect $\Delta_{k-Q}$ was of the order $10^{-3}$, and the defect for the electroneutrality condition was $\sim 10^{-1}$% of the total charge in the polyion. Two cases for the total charge $Np$ in B-DNA$i$ are studied, $Np$ = 240 and $Np$ = 480, to examine the size effect.

**TABLE II: Energy Parameters**

| | $\sigma^a$ | $10^{14}\epsilon^b$ | $Z^c$ |
|---|---|---|---|
| phosphate | 4.0 | 1.0 | −1.0 |
| cation | 4.0 | 1.0 | 1.0 |
| anion | 4.0 | 1.0 | −1.0 |

[a] Unit in angstroms. [b] Unit in erg/molecule. [c] Unit in electronic charge. [d] $u_{ij}(r) = 4\epsilon_{ij}[(\sigma_{ij}/r)^{12} - (\sigma_{ij}/r)^6] + Z_iZ_j/Dr$. [e] $D$ = 78.4.

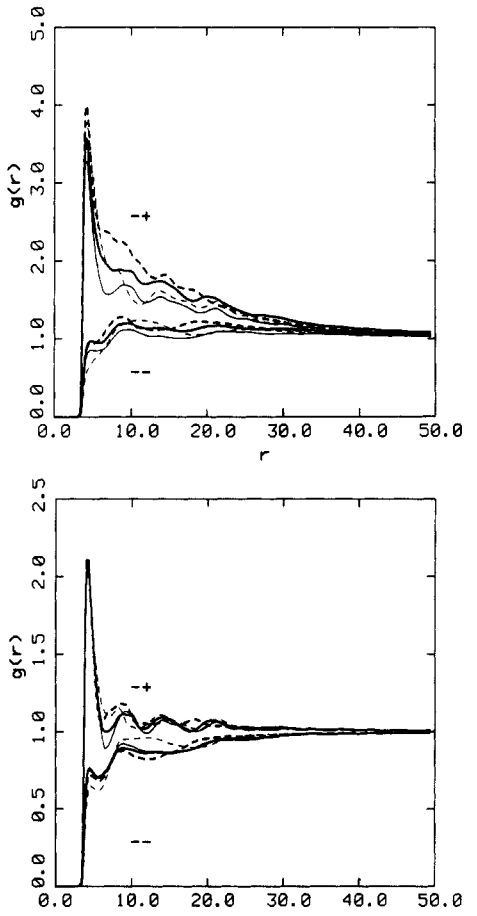


**Figure 2.** Phosphate–small ions correlation functions: thin solid lines, B-DNA0; thick dashed lines, B-DNA1; thick solid lines, B-DNA2; thin dashed lines, B-DNA3. Top: 2.0 M. Bottom: 5.0 M.

*Counter- and Co-ion Distribution around DNA.* Counter- and co-ion distributions around a phosphate are plotted in Figure 2, top and bottom, for 2 and 5 M, respectively, for the various models B-DNA$i$ ($i$ = 0, 1, 2, 3). As discussed in the previous report,[26] the correlation function displays an oscillatory behavior reflecting

(38) Olivares, W.; McQuarrie, D. A. *Biophys. J.* **1975**, *15*, 143; *J. Chem. Phys.* **1976**, *65*, 3604.
(39) Pack, G. R.; Klein, B. J. *Biopolymers* **1984**, *23*, 2801.
(40) Arnott, S.; Hukins, D. W. *Biochem. Biophys. Res. Commun.* **1972**, *47*, 1504.
(41) Hao, M.-H.; Olson, W. K., submitted for publication in *Biopolymers*.

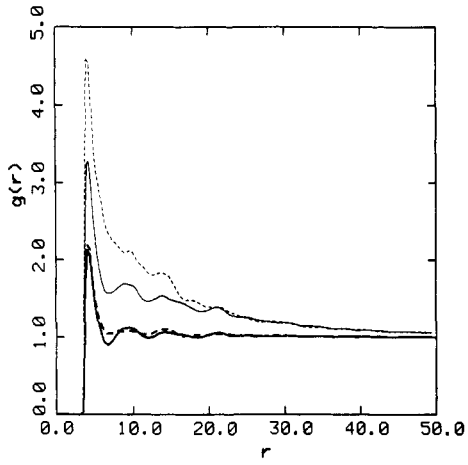


**Figure 3.** Phosphate–counterions correlation functions: solid lines, B-DNA; dashed lines, Z-DNA; thin lines, 2.0 M; thick lines, 5.0 M.

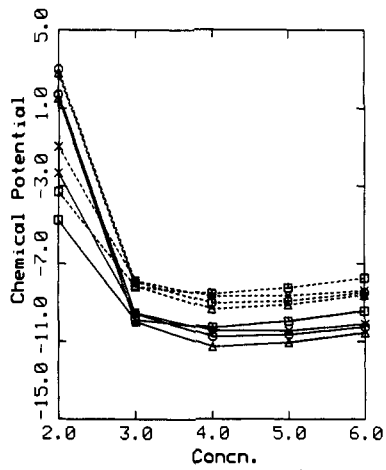


**Figure 4.** $\Delta\mu_p$ for various conformations of B-DNA as a function of salt concentration: squares, B-DNA0; circles, B-DNA1; triangles, B-DNA2; crosses, B-DNA3. Solid lines, $N_p$ = 480; dashed lines, $N_p$ = 240.

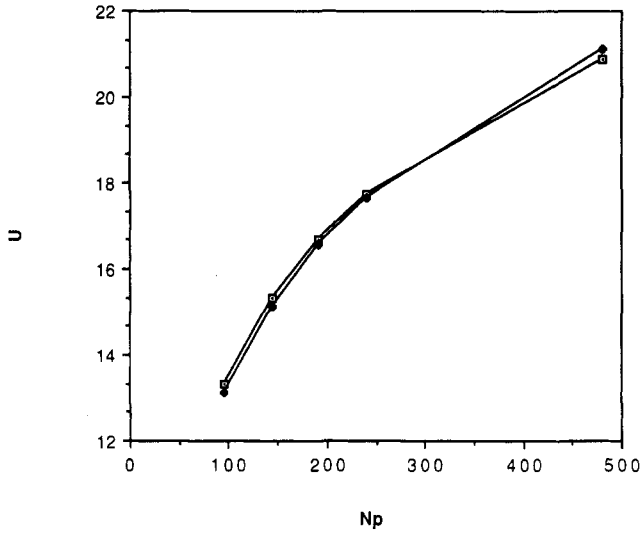


**Figure 5.** $U^D$(B) and $U^D$(Z) as a function of $N_p$: filled diamond, B-DNA; open square, Z-DNA.

the periodic variations of the charge density. For the counterion distribution, the effect of increasing the charge density is similar to the linear charge case. That is, an increase in the charge density causes enhancement of the distribution near phosphates and decreases the rate of decay to unity. The detailed modification of the distribution varies depending on the model. The major aspects persist at higher concentration. However, as the concentration increases and as the screening of the Coulomb interaction increases, the correlation function tends to show characteristics of normal dense fluids.

The most unusual feature of the correlation function is observed in the *co-ion* distribution in the lower concentration regime (Figure 2, top), for which $g(r)$ exceeds unity over a wide range of $r$ before it eventually decays to the bulk value. It physically means that the co-ion concentration close to the phosphates exceeds the bulk values. This tendency becomes more significant when the charge density increases. Since the charge neutrality conditions (zeroth moment), eq 11 and 12, are satisfied, we attribute the behavior to higher moments of the distribution. Whether the behavior is physically correct or results from the approximations involved in the polymer RISM equation is not yet clear. Further investigation by computer simulations is being pursued.

A comparison of Z-DNA and B-DNA phosphate–counterion correlation functions is shown in Figure 3. At the lower concentration (2 M), the counterion concentration at the surface of Z-DNA is considerably higher than that of B-DNA despite the lower linear charge density. The result is generally in accord with the finding by Pack et al.[39] in their generalized Poisson–Boltzmann analysis in spite of the differences in the model and concentrations studied (0.01 M). The behavior is not surprising in light of the results shown for the models of B-DNA with different helix parameters in Figure 2, top. The result implies that the counterion distribution is not solely determined by the axial charge density but depends on a more detailed characterization of the polyion charge distribution.

*Free Energy.* In Figure 4, the excess chemical potential for the B-DNA models calculated with eq 14 is plotted against the concentration of small ions. Various symbols correspond to the different helical parameters for B-DNA described above, and the two types of lines distinguish the number of phosphates in the polyelectrolytes. The most striking feature of the result is the difference in the dependence of the free energy on the charge density between lower and higher concentrations. At lower concentrations the chemical potential for B-DNA0 is lower than those for all other models with higher polyion charge density. The trend is reversed at higher concentration. The transition occurs around 3 M. An important conclusion may be drawn from this result. That is, the salt effect on the conformation is determined not only by the axial charge density of the polyelectrolytes, which is solely a function of $\Delta z_H$ in eq 28, but also by all other helical parameters that affect the polyelectrolyte charge density. It should be noted that the change in the number of phosphates does not alter the qualitative result, although a significant dependence of $\Delta\mu_p$ upon chain length is observed when $N_p$ is changed from 240 to 480. Part of the dependence of $\Delta\mu_{pi}$ upon chain length is cancelled when the *direct* intramolecular contribution is added to $\Delta\mu_{pi}$. Whether the remaining length dependence is real or an artifact of the approximation made is unclear at present.

To investigate the difference in the salt effects on B- and Z-DNA, we define a function $\Delta F_{BZ}$ by the following equation:

$$\Delta F_{BZ} = \Delta\mu_p(\{Z\}) - \Delta\mu_p(\{B\}) + \Delta U_{BZ} \quad (29)$$

$$\Delta U_{BZ} = U^D(\{Z\}) - U^D(\{B\}) \quad (30)$$

where $\Delta\mu_p(\{B\})$ and $\Delta\mu_p(\{Z\})$ are the excess chemical potential for B- and Z-DNA calculated from eq 14 and $U^D(\{B\})$ and $U^D(\{Z\})$ are the direct interaction among phosphates in B- and Z-DNA, which is a sum of pair interactions between phosphates calculated with eq 1. The direct part $\Delta U_{BZ}$ is independent of the salt concentration, giving a contribution of −0.67 kcal/(mol of phosphates), which apparently contradicts the result, +0.69, obtained by Pack et al.[39] The discrepancy is essentially due to the difference in the number of phosphates involved in the calculation. In Figure 5, we plot $U^D(\{B\})$ and $U^D(\{Z\})$ as a function of the number of phosphates, which shows the change in the sign of $\Delta U_{BZ}$ around $N_p$ = 300 (150 base pairs). We suggest a physical explanation for the dependence of $\Delta U_{BZ}$ on the polyion length. For small polyions, $U^D(\{B\})$ and $U^D(\{Z\})$ are dominated by near-neighbor electrostatic interactions. For examples, for Z-DNA the shortest phosphate–phosphate distance between opposite strands is 7.7 Å, while for B-DNA the corresponding value is 11.5 Å. On the other

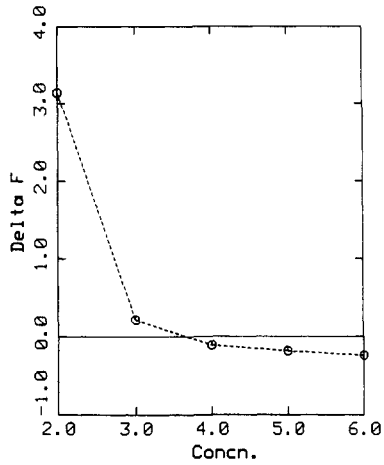


**Figure 6.** $\Delta F_{BZ}$ as a function of salt concentration.

hand, when the polyion is very long, the details of the local charge distribution are less important and the electrostatic potential is dominated by the axial charge density, which is larger for B-DNA than Z-DNA. Since the number of phosphates included in Pack's calculation is 60 (30 base pairs) while it is 480 (240 base pairs) in this study, the opposite sign is attributed to the size dependence of $\Delta U_{BZ}$. In Figure 6, we show the overall free energy change $\Delta F_{BZ}$ associated with the conformational change from B-DNA to Z-DNA. The picture shows qualitatively a similar dependence of $\Delta F_{BZ}$ upon salt concentration as is experimentally observed,[23] exhibiting a transition at ~3.6 mol/L. The concentration of the transition is somewhat higher than that of experiment. Nevertheless the result is encouraging considering the approximations employed and that the model parameters have not been optimized.

Since the more approximate theory by Soumpasis predicts the B–Z transition in a qualitatively similar manner to the polymer RISM result and experiment, it is of interest to comment further on the assumption of the superposition approximation. Comparing eq 9 of ref 25 with eq 26 of the present paper, it appears the superposition approximation is closely related to the following approximations for eq 7 and 10 for the phosphate–small ion correlation function; $\theta_{pi} = 0$ and $\exp(Q_{pi}) = 1 + Q_{pi}$. With respect to the free energy, therefore, the contributions of $\theta_{pi} = 0$ and higher order terms in $Q_{pi}$ cancels when the free energy *difference* between B- and Z-DNA is calculated.

## Concluding Remarks

A RISM theory developed for solvated polymers has been applied to polyelectrolyte solutions. It has been shown that the new approach leads to the same limiting behavior for the chemical potential of polyions at low concentrations as older theories that employ the Mayer-type cluster expansion or the mode expansion method. As an application of the theory, correlation functions between a phosphate and small ions as well as the excess chemical potential of polyions corresponding to different helical forms of DNA have been calculated. From the dependence of the chemical potential upon the charge density of the polyion, it is found that not only the axial charge density of the double helix but also the detailed charge distribution of the polyion affects the conformation. The free energy difference between B- and Z-DNA, which includes the direct part as well as the indirect interaction (salt-induced part), shows a similar dependence upon salt concentration as does the experiment, although the predicted concentration of the transition is somewhat higher than observed experimentally.

There are several directions for refinement or improvement conceivable with respect to the models employed as well as the approximations, which are within the scope of the present method. These include explicit inclusion of the solvent structure, incorporating a more detailed structure of the polyion such as separate correlation functions for the two types of phosphates in Z-DNA, and use of the HNC approximation instead of the PY closure for the phosphate–small ion correlation functions. Improvements in the theory and analysis of solvent effects on diverse superhelical forms of DNA[41] as well as the study of solvent effects on DNA conformation by computer simulation are among our future plans.

*Acknowledgment.* We thank Peter Rossky for helpful comments concerning the manuscript. This work has been supported by a grant (GM-30580) from the NIH, the donors of the Petroleum Research Fund, administered by the American Chemical Society, and the Johnson and Johnson foundation. We thank the National Allocation Committee for the John Von Neumann Center for a grant of supercomputer time. F.H. gratefully acknowledges Supercomputer Fellowship support from Rutgers University and the New Jersey Commission on Science and Technology.

## Appendix

Here we give a proof that $\Delta_{h-Q}$ defined by eq 12 is zero for exact $h_{pi}$ and $Q_{pi}$.

The Fourier transform of eq 9 is

$$Q_{pi}(k) = \sum_j W_p(k)\phi_{pj}(k)\{\delta_{ij} + \rho_j h_{ji}^0(k)\} \tag{A1}$$

where $W_p(k)$, $\phi_{pi}(k)$, and $h_{ji}^0(k)$ are the Fourier transforms of the corresponding functions in real space. Substitution of (21) into (A1) and expansion of $h_{ji}^0(k)$ about small values of $k$ lead to

$$Q_{pi}(k) = W_p(k)\left\{-\beta\frac{4\pi Z_p}{Dk^2}\right\}\left\{Z_i + k^0\left[\sum_j \rho_j Z_j \int h_{ji}^0(r)\,\mathrm{d}r\right] - \frac{k^2}{6}\left[\sum_j \rho_j Z_j \int h_{ji}^0(r) r^2\,\mathrm{d}r\right] + \ldots\right\} \tag{A2}$$

Taking into account the first and second moment conditions for $h_{ij}^0(r)$, namely

$$-Z_i = \sum_j \rho_j Z_j \int h_{ji}^0(r)\,\mathrm{d}r \tag{A3}$$

$$-6Z_i(1/\kappa^2) = \sum_j \rho_j Z_j \int h_{ji}^0(r) r^2\,\mathrm{d}r \tag{A4}$$

(A2) becomes

$$Q_{pi}(k) = W_p(k)\left\{-\frac{4\pi\beta Z_p^2}{Dk^2}\right\}\left\{\frac{Z_i}{\kappa^2}k^2 + (\mathcal{O})k^4 + \ldots\right\} \tag{A5}$$

The expansion of $W_p(k)$ about small $k$ is

$$W(k) = \sum_n\left\{1 - \frac{1}{6}L_n^2k^2 + (\mathcal{O})k^4 + \ldots\right\} = N_p - \frac{1}{6}\{\sum_n L_n^2k^2\} + (\mathcal{O})k^4 + \ldots \tag{A6}$$

Substituting (A6) into (A5), we have

$$Q_{pi}(k) = -\frac{4\pi\beta N_p Z_p Z_i}{D\kappa^2} + (\mathcal{O})k^2 + \ldots \tag{A7}$$

On the other hand, the Fourier transform of $Q(r)$ can be expanded in Taylor series of $k$ as

$$Q_{pi}(k) = \frac{4\pi}{k}\int_0^\infty rQ(r)\sin kr\,\mathrm{d}r = 4\pi\int_0^\infty r^2Q(r)\,\mathrm{d}r - \left\{\frac{4\pi}{6}\int_0^\infty r^4Q(r)\,\mathrm{d}r\right\}k^2 + \ldots \tag{A8}$$

Comparing (A7) and (A8) leads to

$$4\pi\int_0^\infty r^2Q_{pi}(r)\,\mathrm{d}r = -\frac{4\pi\beta N_p Z_p Z_i}{D\kappa^2} \tag{A9}$$

Therefore, we have

$$\sum_i \rho_i Z_i \int_0^\infty Q_{pi}(r)4\pi r^2\,\mathrm{d}r = -\frac{4\pi\beta N_p Z_p \sum_i \rho_i Z_i^2}{D\kappa^2} = -N_p Z_p \tag{A10}$$

In the second equation, we used the definition of $\kappa$. With eq 11 and 12, this proves $\Delta_{h-Q} = 0$.